MIT Open Access Articles

Co-regulation of primary mouse hepatocyte viability and function by oxygen and matrix

Co-regulation of Primary Mouse Hepatocyte Viability and Function by Oxygen and Matrix

Lorenna D. Buck[1], **S. Walker Inman**[1], **Ivan Rusyn**[2], and **Linda G. Griffith**[1]

[1]Department of Biological Engineering, Massachusetts Institute of Technology, 77 Massachusetts Avenue, Cambridge, MA, USA

[2]Department of Environmental Sciences and Engineering, University of North Carolina, Chapel Hill, NC, USA

Abstract

Although oxygen and extracellular matrix cues both influence differentiation state and metabolic function of primary rat and human hepatocytes, relatively little is known about how these factors together regulate behaviors of primary mouse hepatocytes in culture. To determine the effects of pericellular oxygen tension on hepatocellular function, we employed 2 methods of altering oxygen concentration in the local cellular microenvironment of cells cultured in the presence or absence of an extracellular matrix (Matrigel) supplement. By systematically altering medium depth and gas phase oxygen tension, we created multiple oxygen regimes (hypoxic, normoxic, and hyperoxic) and measured the local oxygen concentrations in the pericellular environment using custom-designed oxygen microprobes. From these measurements of oxygen concentrations, we derived values of oxygen consumption rates under a spectrum of environmental contexts, thus providing the first reported estimates of these values for primary mouse hepatocytes. Oxygen tension and matrix microenvironment were found to synergistically regulate hepatocellular survival and function as assessed using quantitative image analysis for cells stained with vital dyes, and assessment of secretion of albumin. Hepatocellular viability was affected only at strongly hypoxic conditions. Surprisingly, albumin secretion rates were greatest at a moderately supra-physiological oxygen concentration, and this effect was mitigated at still greater supra-physiological concentrations. Matrigel enhanced the effects of oxygen on retention of function. This study underscores the importance of carefully controlling cell density, medium depth and gas phase oxygen, as the effects of these parameters on local pericellular oxygen tension and subsequent hepatocellular function are profound.

Keywords

Mouse; hepatocyte; oxygen consumption; static culture; albumin secretion

Correspondence to: Linda G. Griffith, Ph.D. Department of Biological Engineering Massachusetts Institute of Technology 77 Massachusetts Avenue, Room 16-429 Cambridge, MA 02139 griff@mit.edu Phone: (617) 253-0013.

Introduction

In human liver, the oxygen concentration in blood plasma drops as blood flows down the sinusoid, from ~85uM near the portal triad ("periportal" region) to ~45uM at the central vein ("centrilobular" region) (Jungermann and Kietzmann 2000; Martinez et al. 2008). This oxygen gradient contributes to gradients in metabolic activity along the sinusoid in part through the influence of oxygen tension on expression of metabolic enzymes (Allen and Bhatia 2003; Arteel et al. 1999; Bradford et al. 1986; Haussinger 1983; Jungermann and Kietzmann 2000; Nahmias et al. 2006; Pang and Terrell 1981). Hence, local hepatocellular oxygen concentration is an important variable to both predict and control in *in vitro* liver cell culture models of liver function and physiology.

Hepatocytes have a relatively high intrinsic metabolic activity and are typically cultured at high density to maintain cell-cell interactions that regulate differentiated function (Swift and Brouwer 2009; Takehara et al. 1992). The combination of these factors makes virtually every mode of *in vitro* hepatocyte culture diffusion-limited for oxygen, resulting in local pericellular (i.e., located just at the cell surface) oxygen concentrations well below the value of ~185 uM for medium equilibrated with humidified air. Oxygen diffusion gradients can fortuitously result in physiological ranges of oxygen concentration (45-85 uM) at the surface of static monolayer cultures for appropriate combinations of cell density and culture medium depth (Guarino et al. 2004). Conditions for maintaining physiological oxygen concentrations in more complex culture configurations, including 3D bioreactor cultures, can readily be defined provided the cellular oxygen consumption rate is known (Domansky et al. 2009).

While estimates of cellular oxygen consumption derived from perfused liver measurements can be a useful guide for setting up *in vitro* culture conditions (Broetto-Biazon et al. 2008; Matsumara et al. 1986; Matsumara and Thurman 1983; Meren et al. 1986), metabolic rates are typically context-dependent and *in vitro* measurements are desirable to obtain more precise control over culture variables that influence oxygen concentration in the hepatocellular microenvironment. The compendium of measured in vitro hepatocellular oxygen consumption rates under various culture configurations is growing as interest in 3D liver models increases (Domansky et al. 2009; Metzen et al. 1995). Interestingly, despite the widespread use of *in vivo* mouse models for liver biology*, in vitro* oxygen consumption rates for mouse hepatocytes have not been reported, even for the common genetic background C57/Bl6. Because the specific rates of oxygen consumption are generally greater for mouse hepatocytes than those for rat, conditions that are suitable for culture of liver cells from other species may not be optimal for mouse cells (Porter and Brand 1995).

In standard 2D static monolayer cultures, cell density and culture medium depth together determine the oxygen tension at the cell surface as governed by diffusion of oxygen to the metabolically active cell monolayer. Hepatocytes are typically cultured at high confluence (>60,000 cells/cm^2) to preserve cell-cell interactions crucial for phenotypic maintenance, hence cultures maintained under substantial depths of medium risk hypoxia. In rat hepatocyte cell cultures, the onset of hypoxia occurs for medium deeper than 2mm when cultures are confluent (Delraso and Frazier 1999; Sbrana et al. 2012), but the constraints may be more severe for mouse cells, as the in vivo oxygen consumption rates in liver are

higher for mouse than for rat (Harper et al. 1998; Kantrow et al. 1997; Porter and Brand 1995).

Here, we investigate how local pericellular oxygen tension of primary mouse hepatocytes derived from C57 /Bl6 mice depends on cell density, culture medium depth, and extracellular matrix microenvironment under standard incubator conditions (20% oxygen) and conditions of systematically varied gas phase oxygen tension. We employed a constant confluent cell density of 80k cells/cm^2 to preserve hepatocellular function, and used different combinations of medium depth and gas phase oxygen tension to create conditions at the cell surface reflecting three regimes of oxygen concentration: (i) approximately periportal liver zonation (> 60 uM); (ii) approximately centrilobular liver zonation (~50 uM) or (iii) hypoxic (<30 uM), aiming for each regime to create these conditions by two different combinations of variables. We evaluated two independent systems for measuring pericellular oxygen in real-time: a commercially-available system with proprietary sensing plates, and a recently developed custom oxygen microprobe system (Inman 2011). The real-time oxygen measurements from the microprobe system were compared to concentrations inferred to be either hypoxic or normoxic based on reaction with pimonidazole (Hypoxyprobe), and were subsequently used to derive values of cellular oxygen consumption rates. Further, we examined the effects of a well-known modulator of hepatocellular function, extracellular matrix, on cellular responses.

Materials and Methods

Cell Isolation and culture

Primary mouse hepatocytes were isolated using a two-step collagenase perfusion method from 6-12 week old, male C57Bl6 mice based on a protocol described previously with minor changes (Martinez et al. 2010). Livers were excised and dissociated in Isolation/Plating Medium [Williams E base medium (WEM, Sigma) supplemented with 1ug/ml aprotinin (Sigma), 10ug/ml Insulin Transferrin Sodium Selenite (Roche), 2mM Glutamax (Invitrogen), 1X antibiotic/antimycotic (Invitrogen), 10mM HEPES (Sigma), 0.1uM dexamethasone (Sigma), and 10% FBS (Sigma)]. Cell yield and viability were determined using a trypan blue exclusion test. Hepatocytes were further purified by centrifugation using a 45% Percoll solution. Viable hepatocytes were washed twice, subsequently resuspended in Isolation/Plating medium and plated on 12- or 24-well plates pre-coated with 9 ug/cm^2 adsorbed rat tail collagen I (BD) at a density of 8×10^5 cells/cm^2 and a medium depth 1.3mm. Cells were allowed to attach for 4 hours at 37°C and 5% CO$_2$ in a humidified incubator before medium was changed to Maintenance Medium [same as Isolation/Plating Medium, but without FBS] at a medium depth of either 1.3 mm or 2.6 mm. For conditions with Matrigel supplement, Maintenance medium was supplemented with Matrigel (~10 mg/mL) to by adding 3% (v/v) Matrigel to medium to yield a Matrigel concentrion of ~0.3 mg/ml. This was was added 4 hours after plating at a medium depth of either 1.3 mm or 2.6 mm. The 3% Matrigel in solution does not form a gel layer, but provides ECM adhesion molecules that can be bound and organized by cells, and also provides additional growth factors. Medium was replaced on a daily basis. Perfusions yielded initial cell viability above 80% and final viability of around 90% after Percoll purification. For experiments performed

at 10% or 5% oxygen, oxygen tension was controlled by a FormaScientific 3140 incubator connected to a nitrogen gas cylinder. For experiments performed at 40% oxygen, oxygen tension was controlled by a compact oxygen controller (ProOx P110, BioSpherix) connected to a 95% oxygen/5% CO_2 gas cylinder.

Non-Invasive Oxygen Concentration Measurements

Oxygen tension at a fixed height (0.5mm) above the cell surface was measured in a minimally-invasive, real-time manner using 0.5mm diameter optical probes incorporating an oxygen-sensitive ruthenium complex (Inman 2011). A custom-designed culture lid was fabricated to house oxygen sensors such that the height of probes was maintained at 0.5 mm above the surface of the culture dish. Briefly, a lid was fabricated with holes in defined locations centered above each well of a 12-well tissue culture plate. Each hole comprises a threaded pocket, such that when a sensor is fed through the hole, a threaded annulus can be screwed in place to fix the sensor vertically in the hole. Further, there are three posts extending from the bottom surface of the lid which fix the height of the lid relative to the bottom of the culture well. These posts are fastened by screwing them into the bottom of the culture lid. The sensor lid was assembled by feeding each sensor probe through a hole in the lid until it touches cell culture surface at the bottom of the well. Once all of the sensors have been fixed in place, exactly touching the cell culture surface at the bottom of the well, the three posts on the bottom of the culture lid are removed and 0.5 mm thick spacing washers are inserted between the posts and the bottom of the culture lid. With these calibrated washers in place, the probes reside exactly 0.5 mm above the bottom of the wells. Sections were cut in several 12-well plates to verify placement of the probes. (See results section for a schematic.) The error in the probe height is expected to be <±0.05mm, based on a potential 5% error in actual spacer height and less than 1% error that might arise if the probe bends. The probes were calibrated before each use using a 10g/L sodium sulfite solution and air-saturated water as the 0% and 100% air saturation standards, respectively. Real-time oxygen measurements were recorded every 3 minutes for each well in each experiment. All conditions were tested in triplicate from at least 2 independent isolations. Measurements at the 0.5mm height were used to estimate the local cell-surface oxygen concentration by presuming Fickian diffusion in stagnant culture medium, as described in results.

Immunohistochemical Evaluation of Hypoxia

Hypoxia was evaluated by incubating cells with Hypoxyprobe™-1 Plus (Chemicon) for subsequent detection of pimanidazole adducts (Khan et al. 2006). Separate plates were prepared for assessment of hypoxia using cells from the same isolations under which oxygen measurements were collected. Four hours after plating, medium was changed to Maintenance Medium with 200uM Hypoxyprobe™. For conditions with Matrigel™ supplement, medium was changed to 3% (v/v) Matrigel™ in Maintenance Medium with 200uM Hypoxyprobe™ after 4 h. Each condition was tested in duplicate. At 24 h after seeding, cultures were fixed in 2% paraformaldehyde in PBS for 20 minutes and stored at 4°C in PBS until they were stained and imaged. Samples were permeabilized with 1% Triton-X-100 for 5-10 minutes and subsequently rinsed using PBS with 0.1% Tween-20 (PBS-T) (Cosgrove et al. 2008; Walter et al. 2008). Samples were blocked for 30 minutes at room temperature using PBS with 0.1% Tween-20, 1% BSA, and 5% FBS (PBS-TB) added.

Samples were incubated for 1 h with FITC-conjugated MAb1 diluted 1:100 in blocking solution and a 1:1000 dilution of Hoescht 33258 (Invitrogen). Samples were washed once with PBS-TB, resuspended in PBS and imaged using a Compucyte Laser Scanning Cytometer.

Results

Minimally invasive measurements of oxygen in the pericellular environment

We investigated two different methods for real-time assessment of oxygen concentrations in the pericellular microenvironment of hepatocytes maintained in confluent monolayers, using variation in medium depth and gas-phase oxygen: (i) The commercially available PreSens OxoDish and SensorDish Reader oxygen-sensing system, which employs a small disc of sensor material in the middle of the culture surface area in the well covering ~5% of the well surface area in a 24-well plate, allowing real-time reporting of oxygen tension beneath the monolayer of cells plated on top and (ii) a custom probe sensor built in house and described in Materials and Methods.

The real-time oxygen traces for the PreSense OxoDish over the first 48 hr of culture for primary mouse hepatocytes cultured first for 5 hr in 1.3 mm medium depth, then subsequently in either 1.3 mm or 2.6 mm medium depth for an additional 43 hr, are shown in Figure 1. As illustrated by the graphs in Figure 1, after the first and second medium changes, the oxygen concentration reaches steady state within minutes, though a moderate degree of long time-scale variation is seen at the 2.6 mm depth. For cells cultured at the 2.6 mm medium depth, a drop in oxygen concentration at the cell layer after the medium change was expected due to the increased oxygen diffusion distance, and such a drop was observed (from 125 uM to 50 uM, Figure 1). However, for cells cultured at 1.3 mm medium depth, an increase in dissolved oxygen (from 125uM to 150uM) was observed after the medium change. This increase in oxygen suggests the loss of live cells from the surface of the sensor layer during the first medium change, though the steadiness of the oxygen tension at both medium depths following subsequent medium changes suggests cell loss did not occur subsequently.

Phase contrast images showing the edge of the sensor spot demonstrated an area devoid of cells directly around the sensor spot (Figure 1). The sensor spot itself is optically opaque, preventing in-situ phase contrast imaging of cell morphology on the sensor layer, and autofluorescence of the sensor spot similarly inhibits fluorescent imaging of cells above and around the sensor spot. The sensor surface appeared textured under fluorescent imaging, hence offers a different adhesive environment than standard culture plates.

Next, we used a ruthenium-based microprobe system adapted to provide real-time in situ measurement and recording of local oxygen tension in the static culture medium 0.5 mm above cells maintained in a 24-well plate format according to the geometry depicted in Figure 2. The surface area of the probe is <0.1% of the culture surface area of a well in a 12-well plate. Real time oxygen traces over the first 48 hr in culture (Figure 2b) for cells cultured as described above (5 hr culture at 1.3 mm medium depth, followed by medium exchange to defined depth of 1.3 mm or 2.6 mm) exhibit features similar to those shown in

Figure 1: a steady state is reached rapidly after a spike in oxygen tension after medium exchange. Similar behavior is observed if the gas phase oxygen partial pressure is reduced to 10% or 5% (Supplemental Figure 1). The oxygen concentration at the cell monolayer can be calculated from the oxygen concentration recorded by the probes at their location 0.5 mm above the cell monolayer by using a 2-D (radially symmetric) discrete diffusion-reaction equation (see Supplemental Methods). Placement of the 500 um diameter probe slightly distorts the otherwise linear concentration profile of oxygen along its diffusion path, creating a modest depression of oxygen concentration for cells located immediately beneath the probe compared to cells distant from the probe as illustrated by an example concentration profile obtained from the simulation (Figure 2). The magnitude of the offset between the probe measurement and concentration at the surface of the cell monolayer for cells directly under the probe and cells in the bulk far from the probe was determined for a range of placement heights h above the cell surface, medium depths L, and cell consumption rates q_{O2} in order to interpret data subsequently reported herein (see Supplemental Methods). For ease of use, in situ imaging, and minimal footprint on the culture area, the oxygen microprobes were used for subsequent analyses.

Pericellular Oxygen Concentration is a function of Medium Depth and Gas Phase Oxygen Saturation

The real-time measurements (Figure 2, Supplemental Figure 1, and data not shown) indicate that unperturbed cultures maintain a constant oxygen concentration over 20+ hours, after recovery from transients associated with medium changes. Thus, to aid visual comparison of differences between local pericellular oxygen concentrations for cells maintained under different conditions of ambient oxygen, medium depth, and matrix, oxygen concentration measurements obtained every 3 min via microprobes maintained 0.5 mm above the cell surface were averaged over a period of 6 hours during each day (120 measurements) and a pericellular oxygen concentration value associated with each condition and day was derived using the methods described above (see also Supplemental Methods).

The Day 1 oxygen concentration values estimated at the cell surface range dramatically, from 10 uM to 150 uM depending on the medium depth and gas phase oxygen tension. The 20% shallow (1.3 mm depth) oxygen concentration is above 100 uM, slightly greater than physiological oxygen concentrations reported in the periportal region of the liver. 10% shallow (1.3 mm medium depth) oxygen conditions average around 45 uM, at the low end of physiological oxygen concentration in the pericentral region of the *in vivo* mouse liver. In contrast, the 20% deep (2.6 mm) and 5% shallow oxygen conditions result in pericellular oxygen concentrations indicative of borderline or frank hypoxia (10-30 uM). Pericellular oxygen concentration values did not change dramatically over several days of culture (Figure 3a, Supplemental Figure 1).

For most conditions, there was no significant difference in measured pericellular oxygen concentration between hepatocytes cultured in the presence of 3% Matrigel in comparison to those cultured in the absence of 3% Matrigel. Hepatocytes cultured in two different conditions predicted to give comparable pericellular oxygen tensions -- deep medium (20% O_2 with 2.6 mm medium depth) and reduced incubator oxygen (10% O_2, 1.3 mm) – as well

as conditions expected to give very hypoxic conditions (5% O_2, 1.3 mm medium depth) experienced pericellular oxygen concentrations significantly lower than hepatocytes cultured at high oxygen (20% O_2, 1.3 mm) (p<0.001).

The local pericellular oxygen concentrations derived from probe readings are consistent with an independent chemical measure of local tension (Figure 3B). Hypoxyprobe is a water soluble, cell-permeant molecule that forms stable intracellular pimanidazole protein adducts when local intracellular oxygen concentrations fall below 14 uM, a threshold that may be reached for extracellular concentrations above 14 uM due to oxygen gradients from the cell exterior to interior. We therefore stained cells maintained just above and below this threshold. Global intracellular staining indicative of hypoxia was not observed for two different conditions where cells were maintained under conditions where extracellular oxygen was > 100 um (Figure 3b, <5% of image area stained positive). In contrast, global intracellular hypoxyprobe staining was intensely apparent for hepatocytes maintained in four different conditions where extracellular oxygen ranged from 12-29 uM (Figure 3b, 38%-45% of image area positively stained). Significant oxygen diffusion gradients between the cell surface and the intracellular mitochondria can help explain the discrepancy between 25 uM cell surface oxygen and <14 uM intracellular oxygen (Jones and Mason 1978; Jungermann and Kietzmann 2000). Moderate staining was seen in the two conditions which had moderately low extracellular oxygen (37-42 uM), suggesting that there are intracellular regions of these cells with oxygen tensions below 14 uM as well (Figure 3b, 27% of image area positively stained). These data agree with *in situ* studies where gradients in hypoxia staining are seen between the periportal and pericentral regions (Arteel et al. 1997; Arteel et al. 1995). Thus, modulation of either medium depth or incubator oxygen levels can result in comparable oxygen tensions at the cell surface.

Cell Viability and Oxygen Consumption Rates are Affected by Oxygen Concentrations and Extracellular Matrix Supplementation

Primary mouse hepatocytes were plated at a nominal total cell density of 80,000 cells/cm^2 at standard incubator oxygen conditions and 1.3 mm ("shallow") medium depth, and then moved to the trial conditions after 4 hr in culture. Live/dead staining was performed at 24 hr (Day 1) and Day 4 for all oxygen and matrix conditions and then cell density and cell viability were measured using a laser scanning cytometer. As shown in Figure 4, there were no statistical differences in the average total cell numbers between conditions on Day 1, nor significant differences between Days 1 and 4 for any of the conditions. Figure 4 shows composite data from 9 different cell isolations, as not all conditions could be tested for any single isolation due to limitations in the total cells available from a single mouse liver and each condition was run in duplicate or triplicate from at least two separate isolations. Scatter in the initial cell numbers for any given condition on Day 1 reflects variations in the properties of cells isolated on different days. However, not surprisingly, statistically-significant reductions in cell viability were observed for conditions associated with the 10% and 5% incubator oxygen tension conditions (Figure 4b).

The values for oxygen flux at the cell monolayer were calculated for each of the 20%, 10% and 5% oxygen culture conditions on Day 1 (Figure 5a). At standard culture conditions

(20% oxygen, either of 1.3 or 2.6 mm depth) the per-cell oxygen consumption rate is estimated as 380 pmol/million cells/s, based on an average viable cell density of 45,000 cells/ cm^2. Because the cellular oxygen consumption rate leveled off at the highest measured (20%) oxygen conditions, 0th order oxygen consumption kinetics with a constant oxygen consumption rate of 19 pmol/cm^2/s were then used to estimate local oxygen concentrations for hyper-oxygenated conditions (40%) where probe sensitivity was low (Figure 5b). The predictions suggest that the 40%/2.6mm condition should represent an oxygen tension at the cell surface around 200 uM while the 40%/1.3mm medium condition represents a hyperoxic environment with an oxygen tension of approximately 280 uM (Figure 5b).

Effects of oxygen concentration on hepatocyte function

The effects of oxygen on hepatocellular metabolism were assessed by measuring cellular albumin secretion rates over 4 days (Figure 6). On Day 1, differences in albumin production were correlated with oxygen availability, as cells maintained under the higher oxygen conditions (40%/1.3mm, 40%/2.6mm, and 20%/1.3mm medium conditions) produced more albumin than the lower oxygen conditions (20%/2.6mm, 10%/1.3mm and 5%/1.3mm conditions), regardless of the presence or absence of Matrigel supplement (p<0.05). But by day 4, albumin production was significantly greater for conditions with 3% Matrigel in comparison to 0% Matrigel, for all four 40% and 20% oxygen conditions (p<0.05). Interestingly, the 3% Matrigel condition associated with the very highest oxygen tension (40%, 1.3 mm medium depth) resulted in a statically lower set of values for albumin secretion at the later times points (days 2 and 4). These data demonstrate that increased oxygen supply to hepatocytes leads to increased early albumin production, but that ECM and possibly growth factor cues present in Matrigel are important for sustained albumin production, and that a biphasic response of cells to increasing oxygen tension is observed.

Discussion

Despite the widespread use of mice in experimental biology, the basic physiology of primary mouse hepatocytes in culture is relatively less characterized than that of primary liver parenchymal cells from humans and rats. A wide variety of different culture conditions have been used for mouse cultures (Table 1), many of which employ cell densities and culture medium depths that were determined in this study to lead to hypoxia and adverse effects on cell viability (Chandra et al. 2001; Clayton and James E. Darnell 1983; Klaunig et al. 1981; Klingmuller et al. 2006; Leist et al. 1994; Li et al. 2010; Maslansky and Williams 1982; Nemoto and Sakurai 1993; Swift and Brouwer 2009; Swift et al. 2010; Walter et al. 2008). Our findings indicate that both oxygen tension and contributions from a complex ECM additive (Matrigel) regulate hepatocellular function.

In this study we employ 2 methods of altering oxygen availability at the cell surface: changing medium depth and gas-phase oxygen saturation. Medium depth is the most accessible parameter to adjust but adjusting this parameter between otherwise identical culture conditions changes the rate of accumulation of autocrine factors in the media as well as the rate of depletion of media components. Hence, we also employ the complementary approach of changing the incubator oxygen tension. The local oxygen tension in the cellular

microenvironment could also be varied by decreasing (or increasing) the cell density used, which alters the rate per unit area that oxygen is consumed at the cell layer, and thus the local oxygen tension for a given medium depth. However, decreasing the cell density also changes the cell confluence and reduces the number of cell-cell contacts, leading to increased cell spreading more and subsequent changes in differentiation state (Swift and Brouwer 2009). This study demonstrates that both changing the incubator oxygen tension or the medium depth can alter cell-surface oxygen in comparable ways.

Under standard culture conditions (20% O_2 at either 1.3 or 2.6 mm medium depth), our observed per cell oxygen consumption rate of approximately 0.4 nmol/10^6 cells/s (assuming ~1 mg protein/10^6 cells) is comparable to those rates measured in perfused livers and mitochondrial preparations from mice, which range from 0.3-0.8 nmol/10^6 cells/s (Broetto-Biazon et al. 2008; Matoba et al. 2006; Porter and Brand 1995). We posit this is the first reported value of per-cell oxygen consumption from *in vitro* mouse hepatocyte cultures. These values are also of a similar magnitude to those reported for rat and human *in vitro* hepatocyte cultures, which range from 0.2-0.7 nmol/10^6 cells/s (Broetto-Biazon et al. 2008; Domansky et al. 2009; Matsumara et al. 1986; Metzen et al. 1995). While mouse hepatocytes are found to be more highly metabolic than rat and human hepatocytes when tested in a single lab, there is a wide range of variability in measured oxygen consumption rates across labs, making it difficult to definitively assess how our observed consumption rates would compare to primary rat hepatocytes cultured similarly.

The values we observed for albumin secretion under standard culture conditions (between 250-380 ug albumin/10^6 cells/day for all timepoints for hepatocytes plated at 20% O_2/1.3mm medium depth) are higher than those previously reported for mouse hepatocytes (which range between 1-250 ug albumin/10^6 cells/day), although medium depth is rarely specified in the literature (He and Feng 2000; Higuchi et al. 2006; Iacob et al. 2011; Sakai et al. 2002; Sharma et al. 2009; Takagi et al. 2012). We also observe significantly increased albumin production and maintenance at 40% incubator oxygen (between 300-1000 ug albumin/10^6 cells/day). Previous studies with primary rat hepatocytes under supraphysiological oxygen have also shown significant improvement in metabolism and drug clearance (Kidambi et al. 2009). We also observe that at hyperoxic levels, albumin production plateaus, as demonstrated from the 40% shallow condition (40% O_2/1.3mm medium depth), which has either the same or lower albumin secretion rates than the 40% deep condition (40% O_2/2.6mm medium depth). This behavior suggests that there is a supra-physiological oxygen concentration value at which hepatocytes no longer benefit and could represent the point at which the effects of oxidative stress begin, as previously reported (Martin et al. 2002).

It is well established that primary hepatocytes cultured on or under Matrigel (i.e. sandwich configuration) retain cell polarity and maintain higher levels of albumin secretion (Dunn et al. 1989; Dunn et al. 1991; Moghe et al. 1996). In this study, Matrigel plays a large role in the maintenance of albumin secretion through Day 4, even when used as a medium supplement (concentrations as low as 3%) added solely on Day 0. By regulating matrix cues in conjunction with oxygen availability, primary mouse hepatocytes can be maintained in culture with high levels of function.

Supplementary Material

Refer to Web version on PubMed Central for supplementary material.

Acknowledgments

References

Arteel GE, Iimuro Y, Yin M, Raleigh JA, Thurman RG. Chronic enteral ethanol treatment causes hypoxia in rat liver tissue in vivo. Hepatology. 1997; 25(4):920–926. [PubMed: 9096598]

Arteel GE, Thurman RG, Yates JM, Raleigh JA. Evidence that hypoxia markers detect oxygen gradients in liver: pimonidazole and retrograde perfusion of rat liver. British Journal of Cancer. 1995; 72:889–895. [PubMed: 7547236]

Broetto-Biazon AC, Bracht F, Bracht L, Kelmer-Bracht AM, Bracht A. Transformation and action of extracellular NAD+ in perfused rat and mouse livers. Acta Pharmacol Sin. 2008; 30(1):90–97. [PubMed: 19079292]

Chandra P, Lecluyse E, Brouwer K. Optimization of culture conditions for determining hepatobiliary disposition of taurocholate in sandwich-cultured rat hepatocytes. In Vitro Cellular & Developmental Biology - Animal. 2001; 37(6):380–385. [PubMed: 11515972]

Clayton DF, James E, Darnell J. Changes in Liver-Specific Compared to Common Gene Transcription During Primary Culture of Mouse Hepatocytes. Mol Cell Biol. 1983; 3(9):1552–1561. [PubMed: 6633533]

Cosgrove BD, Cheng C, Pritchard JR, Stolz DB, Lauffenburger DA, Griffith LG. An Inducible Autocrine Cascade Regulates Rat Hepatocyte Proliferation and Apoptosis Responses to Tumor Necrosis Factor-alpha. Hepatology. 2008; 48(1):276–288. [PubMed: 18536058]

Delraso NJ, Frazier JM. Effect of culture conditions prior to exposure on cadmium cytotoxicity in primary rat hepatocytes. Toxicology Mechanisms and Methods. 1999; 9(2):97–114.

Domansky K, Inman W, Serdy J, Dash A, Lim MHM, Griffith LG. Perfused multiwell plate for 3D liver tissue engineering. Lab on a Chip. 2009; 10(1):51–58. [PubMed: 20024050]

Dunn JC, Yarmush ML, Koebe HG, Tompkins RG. Hepatocyte function and extracellular matrix geometry: long-term culture in a sandwich configuration [published erratum appears in FASEB J 1989 May;3(7):1873]. FASEB J. 1989; 3(2):174–177. [PubMed: 2914628]

Dunn JCY, Tompkins RG, Yarmush ML. Long-term in vitro function of adult hepatocytes in a collagen sandwich configuration. Biotechnol Prog. 1991; 7(3):237–245. [PubMed: 1367596]

Guarino RD, Dike LE, Haq TA, Rowley JA, Pitner JB, Timmins MR. Method for determining oxygen consumption rates of static cultures from microplate measurements of pericellular dissolved oxygen concentration. Biotechnology and Bioengineering. 2004; 86(7):775–787. [PubMed: 15162453]

Harper M-E, Monemdjou S, Ramsey JJ, Weindruch R. Age-related increase in mitochondrial proton leak and decrease in ATP turnover reactions in mouse hepatocytes. American Journal of Physiology - Endocrinology And Metabolism. 1998; 275(2):E197–E206.

Inman, SW. Integration of real time oxygen measurements with a 3D perfused tissue culture system. Massachusetts Institute of Technology; Cambridge: 2011.

Jones DP, Mason HS. Gradients of O2 concentration in hepatocytes. Journal of Biological Chemistry. 1978; 253(14):4874–4880. [PubMed: 209020]

Jungermann K, Kietzmann T. Oxygen: Modulator of Metabolic Zonation and Disease of the Liver. Hepatology. 2000; 31(2):255–260. [PubMed: 10655244]

Kantrow SP, Taylor DE, Carraway MS, Piantadosi CA. Oxidative Metabolism in Rat Hepatocytes and Mitochondria during Sepsis. Archives of Biochemistry and Biophysics. 1997; 345(2):278–288. [PubMed: 9308900]

Khan Z, Michalopoulos GK, Stolz DB. Peroxisomal Localization of Hypoxia-Inducible Factors and Hypoxia-Inducible Factor Regulatory Hydroxylases in Primary Rat Hepatocytes Exposed to Hypoxia-Reoxygenation. Am J Pathol. 2006; 169(4):1251–1269. [PubMed: 17003483]

Kidambi S, Yarmush RS, Novik E, Chao P, Yarmush ML, Nahmias Y. Oxygen-mediated enhancement of primary hepatocyte metabolism, functional polarization, gene expression, and drug clearance. Proceedings of the National Academy of Sciences. 2009; 106(37):15714–15719.

Klaunig JE, Goldblatt PJ, Hinton DE, Lipsky MM, Trump BF. Mouse Liver Cell Culture. II. Primary Culture. In Vitro. 1981; 17(20):926–934. [PubMed: 7309042]

Klingmuller U, Bauer A, Bohl S, Nickel PJ, Breitkopf K, Dooley S, Zellmer S, Kern C, Merfort I, Sparna T. Primary mouse hepatocytes for systems biology approaches: a standardized in vitro system for modelling of signal transduction pathways. Systems Biology, IEE Proceedings. 2006; 153(6):433–447. others.

Leist M, Gantner F, Bohlinger I, Germann PG, Tiegs G, Wendel A. Murine Hepatocyte Apoptosis Induced In Vitro and In Vivo by TNF-alpha Requires Transcriptional Arrest. J Immunol. 1994; 153(4):1778–1788. [PubMed: 8046244]

Li, W-C.; Ralphs, KL.; Tosh, D. Isolation and Culture of Adult Mouse Hepatocytes. In: Ward, A.; Tosh, D., editors. Mouse Cell Culture: Methods and Protocols: Springer Science+Business Media. 2010. p. 185-196.

Martin H, Sarsat JP, Lerche-Langrand C, Housset C, Balladur P, Toutain H, Albaladejo V. Morphological and Biochemical Integrity of Human Liver Slices in Long-Term Culture: Effects of Oxygen Tension. Cell Biology and Toxicology. 2002; 18(2):73–85. [PubMed: 12046692]

Martinez I, Nedredal G, Oie C, Warren A, Johansen O, Le Couteur D, Smedsrod B. The influence of oxygen tension on the structure and function of isolated liver sinusoidal endothelial cells. Comparative Hepatology. 2008; 7(1):4. [PubMed: 18457588]

Martinez SM, Bradford BU, Soldatow VY, Kosyk O, Sandot A, Witek R, Kaiser R, Stewart T, Amaral K, Freeman K. Evaluation of an in vitro toxicogenetic mouse model for hepatotoxicity. Toxicol Appl Pharmacol. 2010; 249(208-216) others.

Maslansky CJ, Williams GM. Primary Cultures and the Levels of Cytochrome P450 in Hepatocytes from Mouse, Rat, Hamster, and Rabbit Liver. In Vitro. 1982; 18(8):683–693. [PubMed: 7129482]

Matoba S, Kang J-G, Patino WD, Wragg A, Boehm M, Gavrilova O, Hurley PJ, Bunz F, Hwang PM. p53 Regulates Mitochondrial Respiration. Science. 2006; 312(5780):1650–1653. [PubMed: 16728594]

Matsumara T, C. KF, Meren H, Thurman RG. O2 uptake in periportal and pericentral regions of liver lobule in perfused liver. Am J Physiol Gastrointest Liver Physiol. 1986; 250:G800–G805.

Matsumara T, Thurman RG. Measuring rates of O2 uptake in periportal and pericentral regions of the liver lobule: stop-flow experiments with perfused liver. Am J Physiol Gastrointest Liver Physiol. 1983; 244(7):G656–G659.

Meren H, Matsumara T, FC K, Thurman RG. Relationship between oxygen tension and oxygen uptake in the perfused rat liver. Adv Exp Med Biol. 1986; 200:467–476. [PubMed: 3799338]

Metzen E, Wolff M, Fandrey J, Jelkmann W. Pericellular PO2 and O2 consumption in monolayer cell cultures. Respiration Physiology. 1995; 100:101–106. [PubMed: 7624611]

Moghe PV, Berthiaume F, Ezzell RM, Toner M, Tompkins RG, Yarmush ML. Culture matrix configuration and composition in the maintenance of hepatocyte polarity and function. Biomaterials. 1996; 17(3):373–385. [PubMed: 8745335]

Nemoto N, Sakurai J. Activation of Cyp1a1 and Cyp1a2 Genes in Adult Mouse Hepatocytes in Primary Culture. Cancer Science. 1993; 84(3):272–278.

Porter RK, Brand MD. Cellular oxygen consumption depends on body mass. Regulatory Integrative Comp. Physiol. 1995; 38:R226–R228.

Sbrana, T.; Ahluwalia, A.; Balls, M.; Combes, RD.; Bhogal, N. New Technologies for Toxicity Testing. Springer; US: 2012. Engineering Quasi-Vivo® in Vitro Organ Models; p. 138-153.

Swift B, Brouwer KLR. Influence of Seeding Density and Extracellular Matrix on Bile Acid Transport and Mrpr Expression in Sandwich-Cultured Mouse Hepatocytes. Molecular Pharmaceutics. 2009; 7(2):491–500. [PubMed: 19968322]

Swift B, Pfeifer ND, Brouwer KLR. Sandwich-cultured hepatocytes: an in vitro model to evaluate hepatobiliary transporter-based drug interactions and hepatotoxicity. Drug Metabolism Reviews. 2010; 42(3):446–471. [PubMed: 20109035]

Takehara T, Matsumoto K, Nakamura T. Cell Density-Dependent Regulation of Albumin Synthesis and DNA Synthesis in Rat Hepatocytes by Hepatocyte Growth Factor. J Biochem. 1992; 112(3): 330–334. [PubMed: 1429519]

Walter D, Schmich K, Vogel S, Pick R, Kaufmann T, Hochmuth FC, Haber A, Neubert K, McNelly S, Weizsacker Fv. Switch from type II to I Fas/CD95 death signaling upon in vitro culturing of primary mouse hepatocytes. Hepatology. 2008; 48(6):1942–1953. others. [PubMed: 19003879]
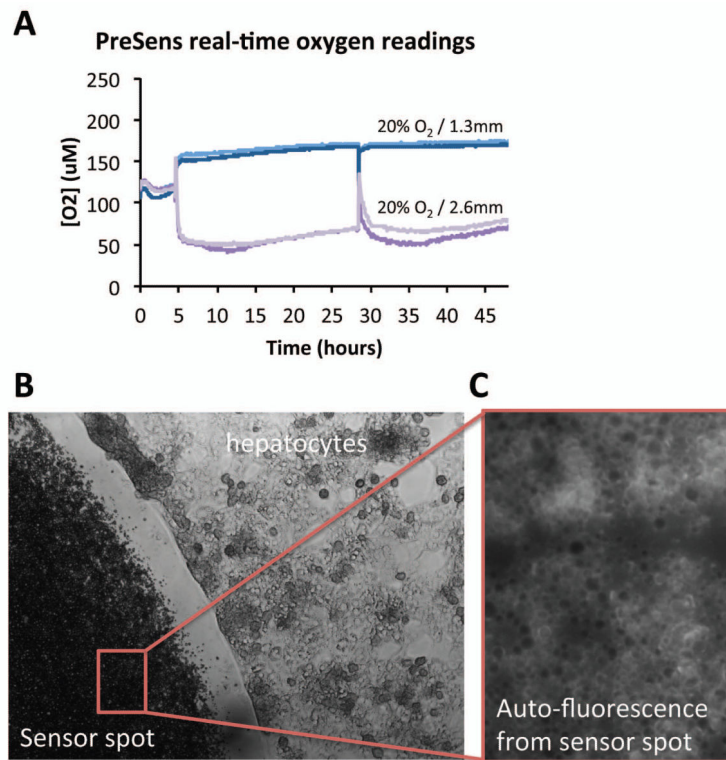
Figure 1.
Evaluation of PreSens OxoDish + SensorDish Reader. A. Real-time oxygen traces, recorded every 3 minutes over the first 48 h of culture for primary mouse hepatocytes cultured first for 5 h at 1.3mm medium depth, then subsequently either 1.3 mm or 2.6 mm medium depth. B. Representative phase contrast image of hepatocytes cultured adjacent to the edge of the sensor spot, after 48 h of culture. C. Representative fluorescent image of sensor surface on OxoDish culture plate.
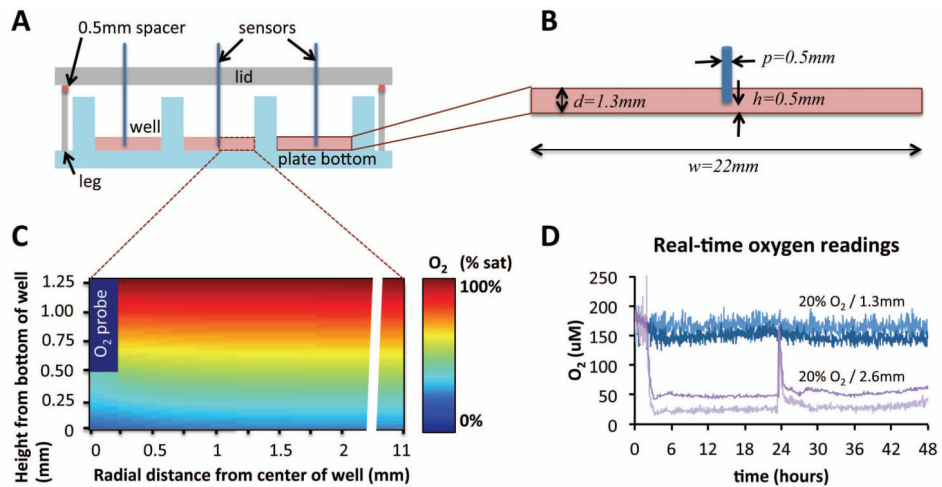
Figure 2.
Precise placement of oxygen sensors allow for real-time measurement of oxygen concentration near the cell surface. A. Schematic diagram showing a cross-section of the sensor lid with integrated sensors in a 12-well culture plate. Once the probes are secured flush with the bottom of the plate, 0.5 mm spacers are added to the legs to raise the sensors 0.5 mm above the well bottom. B. Diagram showing the cross-section of a single culture well with a 0.5 mm diameter probe situated in the center of the well, 0.5 mm above the well bottom, with 1.3 mm medium depth. C. A discrete diffusion-reaction model showing oxygen concentration in a radial cross-section of a culture well with the oxygen probe placed in the center, assuming steady-state oxygen consumption along the bottom of the well. D. Real-time oxygen traces, recorded every 3 minutes over the first 48 h of culture for primary mouse hepatocytes cultured first for 3 h at 1.3mm medium depth, then subsequently either 1.3 mm or 2.6 mm medium depth.
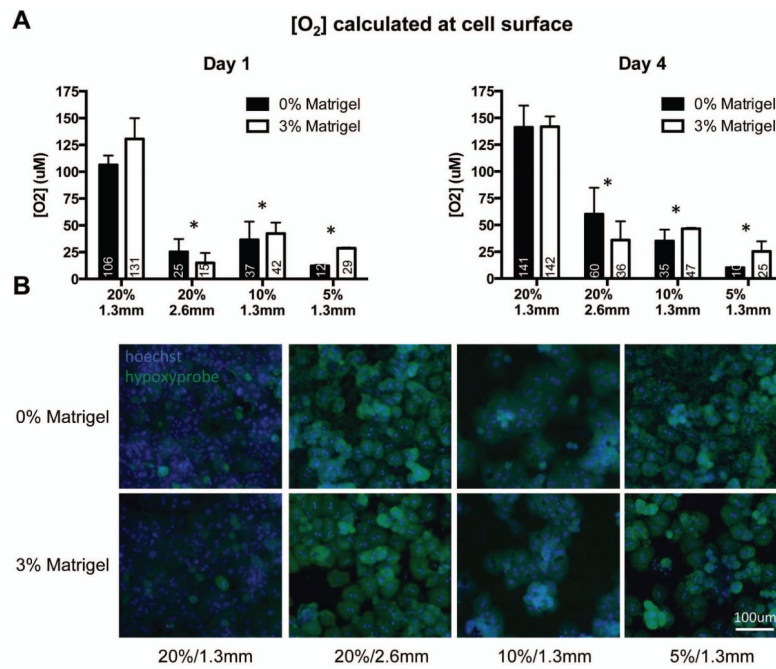
Figure 3.
Pericellular oxygen concentration is a function of medium depth and gas phase oxygen saturation. A. Oxygen concentration at the cell surface, calculated from averaging probe measurements for Days 1 and 4. Data * indicates statistically significant difference from 20 % / 1.3 mm condition (p <0.001, n=2). B. Representative images of hoescht (blue) and hypoxyprobe (green) staining 24 h after initial seeding. All images have common exposure intensities and thresholding. Non-specific staining of dead cells is observed in all conditions.
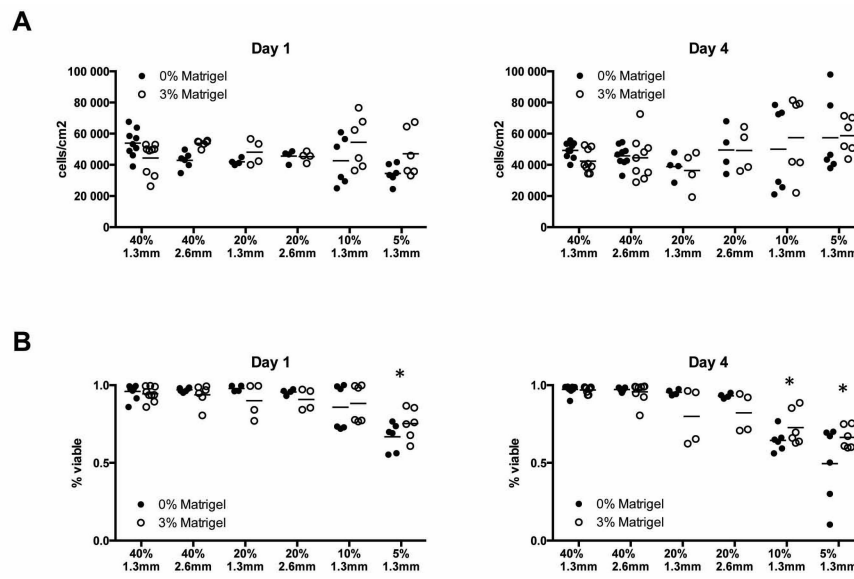
Figure 4.
Results of quantitative imaging following Hoechst/EtBr staining on Days 1 and 4. **A.** Dot plot showing density of viable cells calculated for each biological replicate, as a function of gas-phase oxygen saturation and medium depths. **B.** Percentage of live cells, defined as the fraction of non-EtBr stained nuclei. * indicates statistically significant difference from 20 % / 1.3 mm condition (p <0.05).
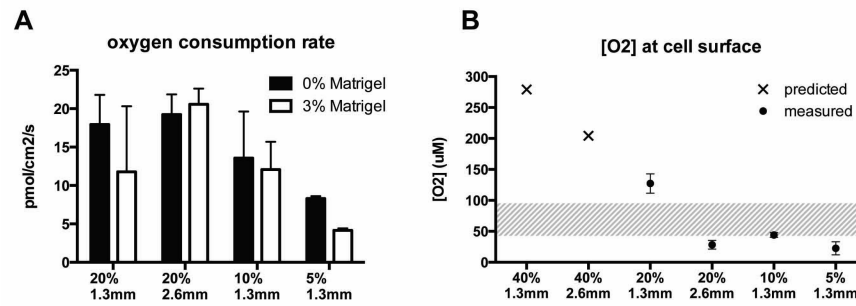
Figure 5.
Modeling and predicting steady-state oxygen consumption based on experimental data. **A.** Day 1 oxygen consumption rates, calculated from cell-surface oxygen measurements and gas-phase oxygen saturation. **B.** 0th order oxygen diffusion model fit to the Day 1 experimental averages of oxygen concentration at the cell surface.
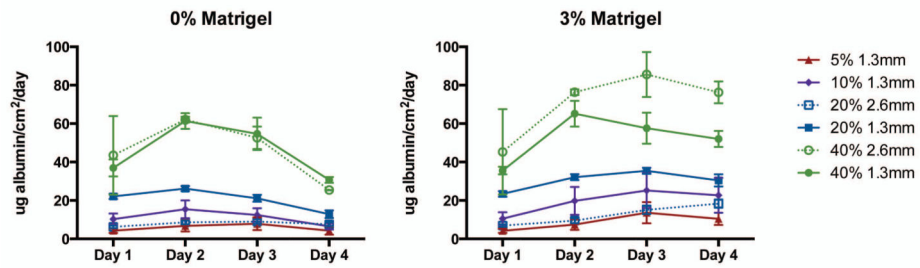
Figure 6.
Albumin secretion is influenced at early timepoints by oxygen and at late timepoints by Matrigel and oxygen. Conditioned media from hepatocyte cultures was collected/replaced with fresh medium ever 24 hours and albumin was quantified via ELISA. Standards and samples were tested in triplicate. All conditions shows statistically significant difference from 20% O_2/1.3mm conditions except * ($p<0.05$, $n>2$).

Table I

Compendium of Geometric and Cell Density Culture Conditions for Mouse Hepatocytes

Reference	Total Cell Number	Plate Type	Medium Volume (ml)	Cell Density ($\times 10^3$ cells/cm^2)	Medium Depth (mm)
(Clayton and James E. Darnell 1983)	10M	150mm plate	15	56.6	0.8
	10M	150mm plate	20	56.6	1.1
(Leist et al. 1994)	80k	24 well plate	0.2	40.0	1.0
(Nemoto and Sakurai 1993)	15M	100ml dish	10	63.7	1.3
(Li et al. 2010)	600k	35mm dish	1.5	62.5	1.6
(Walter et al. 2008)	5M	9cm diameter	10	79.4	1.6
(Swift et al. 2010)	1.25M	6 well plate	1.5	130.2	1.6
	350k	24 well plate	0.5	175.0	2.5
(Klaunig et al. 1981)	1M	25cm2 flask	5	40.0	2.0
(Maslansky and Williams 1982)	500k	25cm2 flask	7	20.0	2.8
(Swift and Brouwer 2009)	1M	6 well plate	3	104.2	3.1
(Chandra et al. 2001)	1.5M	6 well plate	3	156.3	3.1
(Klingmuller et al. 2006)	1M	6 well plate	3	104.2	3.1